J. Mol. Biol. (1997) 267, 47–59

JMB

# DNA-melting at the *Bacillus subtilis* Flagellin Promoter Nucleates Near −10 and Expands Unidirectionally

**Ya-Fen Chen and John D. Helmann***

*Section of Microbiology, Cornell University, Ithaca, NY 14853, USA*

**Corresponding author*

A central step in promoter activation by RNA polymerase (RNAP) is the localized separation of the DNA strands to form the transcription bubble. We have used potassium permanganate footprinting to monitor DNA strand-separation by the *Bacillus subtilis* $\sigma^D$ RNAP at the strong promoter, $P_{hag}$, directing transcription of flagellin. The susceptibility of individual thymine bases to permanganate oxidation is influenced by temperature, $Mg^{2+}$, nucleotides, and the RNAP δ subunit. In the absence of δ, $\sigma^D$ RNAP establishes a partially opened complex even at 0°C with permanganate reactivity localized between −11 and −4 ($RP_{-4}$). The region of strand separation expands to near −1 at 20°C ($RP_{-1}$) and to +3 at 40°C ($RP_{+3}$). The δ subunit inhibits the downstream propagation of the transcription bubble and thereby increases the concentration of early intermediates in the melting pathway. Indeed, $E\delta\sigma^D$ forms a distinct nucleated complex ($RP_n$) at 0°C with a structural distortion localized to an AT base step within the −10 element. We propose a model for promoter melting in which strand separation nucleates within the conserved −10 consensus and subsequently propagates downstream. $Mg^{2+}$ and nucleoside triphosphates (NTPs) favor the downstream propagation of the transcription bubble and strongly stimulate the $RP_{-1}$ to $RP_{+3}$ conversion. The NTP effects are apparently mediated by binding of substrate to the initiating NTP site: purines are more effective than pyrimidines and GMP alone can greatly increase the level of DNA-melting. The binding of substrates, but not $Mg^{2+}$ alone, can effectively overcome the anti-melting effect of δ.

© 1997 Academic Press Limited

*Keywords:* RNA polymerase; sigma; DNA-melting; promoter; open-complex

## Introduction

The selectivity of transcription initiation results from a complex series of interactions between bacterial RNA polymerase (RNAP) and the promoter (Leirmo & Record, 1990; McClure, 1985; von Hippel *et al.*, 1984). RNAP first interacts with the promoter to form a closed complex ($RP_c$) in which the DNA strands are not yet melted. Typically, formation of this recognition complex is driven by favorable electrostatic interactions between RNAP and DNA and by sequence-specific interactions between σ and bases in the −35 and −10 recognition elements (deHaseth & Helmann, 1995; Leirmo & Record, 1990; Chamberlin, 1988). $RP_c$ is in equilibrium with other binary RNAP-promoter complexes, most notably the strand-separated open complex, $RP_0$, in which 12 to 18 bp of DNA are melted. This site-specific DNA-melting reaction is favored by elevated temperature and appears to involve contacts between the associated σ subunit and the non-template strand of the transcription bubble (deHaseth & Helmann, 1995; Helmann, 1994; Buckle *et al.*, 1991). $RP_0$ is competent to bind the nucleoside triphosphate (NTP) substrates required for the initiation and elongation of an RNA chain. The initial stages of RNA synthesis are not very processive and short RNA chains are frequently released in a process termed abortive transcription (Carpousis & Gralla, 1980; Munson & Reznikoff, 1981). Ultimately, RNAP clears the promoter region and establishes a stable and highly

Present address: Ya-Fen Chen, Stanford University Medical Center, Grant S380, Stanford, CA 94305-5119, USA.

Abbreviations used: RNAP, RNA polymerase; PCR, polymerase chain reaction; NTP, nucleoside triphosphate; NMP, nucleoside monophosphate; nt, non-template; t, template.

0022–2836/97/110047–13 $25.00/0/mb960853

© 1997 Academic Press Limited

processive elongation complex ($RP_e$; Arndt & Chamberlin, 1990; Krummel & Chamberlin, 1992). Promoter clearance is accompanied by a large conformational change in the RNAP-DNA complex and the concomitant release of the σ subunit (Krummel & Chamberlin, 1989).

Multiple intermediates have been described in the pathway leading to the formation of the open complex. *Escherichia coli* RNAP forms a second closed complex, designated $RP_i$, which has a DNase I footprint extending to the region of transcription initiation, but which has not yet melted the transcription bubble (Mecsas *et al.*, 1991; Schickor *et al.*, 1990; Spassky *et al.*, 1985). This is the dominant binary complex near 20°C at *lac*UV5, whereas $RP_c$ predominates at 4°C. The $RP_c$ to $RP_i$ transition is accompanied by a large negative heat capacity change consistent with a conformational change resulting in the burial of hydrophobic surface (Leirmo & Record, 1990). The $RP_i$ to $RP_o$ transition has a large positive enthalpy and correlates with DNA-melting as judged by the increased accessibility of bases within the transcription bubble to single-strand specific chemical modifications (Buckle & Buc, 1994). At most, *E. coli* promoters analyzed to date, the DNA-melting process is highly cooperative with concurrent melting throughout the transcription bubble (Buc & McClure, 1985; Cowing *et al.*, 1989; Grimes *et al.*, 1991; Kirkegaard *et al.*, 1983). However, by altering reaction conditions it is sometimes possible to visualize additional intermediates. For example, studies with λ $P_R$ indicate that $Mg^{2+}$ binds to an initially formed open complex ($RP_{o1}$) and stimulates formation of the fully strand-separated intermediate ($RP_{o2}$; Craig *et al.*, 1995; Suh *et al.*, 1992, 1993).

Previously, we investigated the pathway of promoter activation by *Bacillus subtilis* RNAP carrying the major vegetative σ subunit, $\sigma^A$. Although similar in many respects to the *E. coli* enzyme, *B. subtilis* $\sigma^A$ RNAP displays a more stringent promoter selectivity (Voskuil *et al.*, 1995; Whipple & Sonenshein, 1992) and often does not form stable open complexes. Indeed, at many *B. subtilis* promoters only clearance is irreversible: all of the preceding intermediates in initiation are interconvertible, depending on reaction conditions (Whipple & Sonenshein, 1992). In addition, *B. subtilis* RNAP contains an additional dissociable subunit, δ (Pero *et al.*, 1975). Thus, we must distinguish between core ($\beta\beta'\alpha_2$ or E), core + δ($\beta\beta'\alpha_2\delta$ or Eδ), core + σ($\beta\beta'\alpha_2\sigma$ or Eσ), and the true holoenzyme, core + σ + δ($\beta\beta'\alpha_2\delta\sigma$ or Eδσ). While σ determines promoter specificity, δ plays an important role in decreasing the association of RNAP with weak promoters and non-promoter DNA and thereby augments the selectivity of transcription (Achberger & Whiteley, 1981; Achberger *et al.*, 1982; Dobinson & Spiegelman, 1987; Hilton & Whiteley, 1985; Juang & Helmann, 1994a). Indeed, δ can either increase or decrease transcription. At low temperatures δ inhibits transcription by opposing the rate-limiting process of promoter-melting (Juang & Helmann, 1994a, 1995). This is evident even at strong promoters (e.g. $P_{ilv}$ or $P_{trnS}$) which bind Eδ$\sigma^A$ even at 4°C as judged by DNase I protection. Conversely, at temperatures above 30°C δ stimulates transcription severalfold by increasing the ability of RNAP to initiate new chains (Juang & Helmann, 1994a). The mechanism of this stimulation is not clear, but it is postulated to involve the displacement of RNA from inhibited RNAP-RNA complexes by an unstructured, polyanionic region in the carboxy terminus of δ (López de Saro *et al.*, 1995).

In this study, we define intermediates in transcription initiation by *B. subtilis* RNAP bearing an alternate σ subunit, $\sigma^D$, specifying transcription initiation at promoters of the flagellar regulon (Helmann, 1991). We demonstrate that temperature, δ protein, $Mg^{2+}$, and NTPs all affect the nature and extent of strand separation. Our results lead us to propose a pathway of promoter activation involving an initial nucleated complex ($RP_n$), two intermediate open complexes ($RP_{-4}$ and $RP_{-1}$), and a fully extended open complex ($RP_{+3}$) stabilized by $Mg^{2+}$ and NTPs. $RP_n$ appears to have a highly localized distortion within the −10 element which is postulated to initiate the melting process. Thus, promoter melting by *B. subtilis* RNAP appears to occur in discrete steps rather than in a concerted manner.

## Results

We have used DNase I and the single-strand selective reagent potassium permanganate to visualize complexes between $\sigma^D$ RNAP and the strong flagellin promoter, $P_{hag}$ (Mirel & Chamberlin, 1989). We demonstrated previously that $P_{hag}$ contains an upstream promoter element (UP element) which binds the α subunits of RNAP and stimulates transcription approximately 30-fold (Fredrick *et al.*, 1995). We now report that melting of $P_{hag}$ nucleates near the conserved −10 element and propagates downstream in an essentially unidirectional manner. By varying the reaction conditions (e.g. temperature, $Mg^{2+}$, δ protein, and substrates) we can visualize several intermediates in the promoter melting process. For purposes of presentation, we designate these as $RP_n$, $RP_{-4}$, $RP_{-1}$, and $RP_{+3}$ depending on the boundaries of permanganate reactivity. These appear to represent discrete intermediates, rather than points along a continuum, since each is visualized under multiple conditions and persists over a range of temperatures. However, our results do not rule out additional intermediates not detected in this analysis.

### DNase I footprinting of E(δ)$\sigma^D$ RNAP at $P_{hag}$

In our initial studies (Figure 1), we reconstituted $\sigma^D$ RNAP from core enzyme which contained near-stoichiometric levels of δ, indicated as E(δ) (Chen & Helmann, 1995). We used DNase I footprinting to analyze complexes between E(δ)$\sigma^D$ and

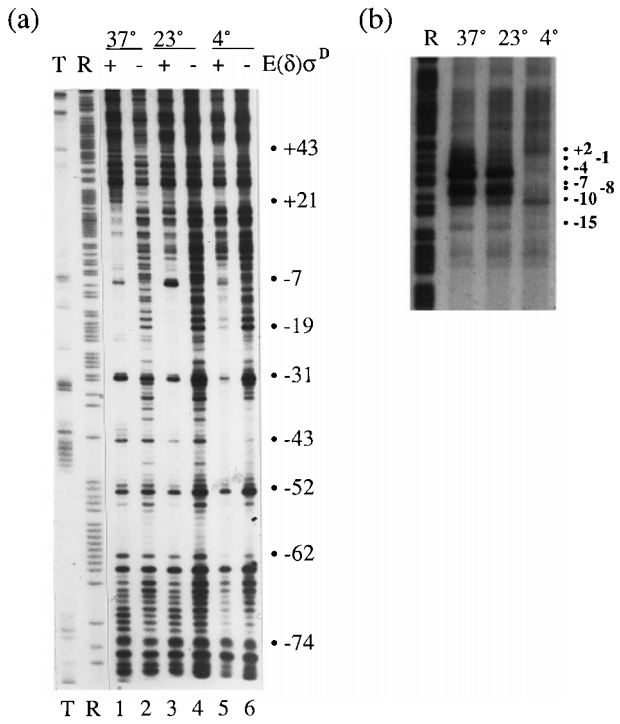



**Figure 1.** Footprinting of $E(\delta)\sigma^D$ at $P_{hag}$ as a function of temperature. (a) DNase I cleavage of $P_{hag}$ on the non-template strand (nt) at 37°C (lanes 1 and 2), 23°C (lanes 3 and 4), and 4°C (lanes 5 and 6). Lanes 1, 3, and 5, $E(\delta)\sigma^D$ holenzyme; lanes 2, 4, and 6, no protein control. ane T, thymine specific chemical sequencing ladder. Lane R, A + G chemical sequencing ladder. (b) Potassium permanganate reactivity of $E(\delta)\sigma^D$ binary complexes at $P_{hag}$ (nt) as a function of temperature. lane 1, 37°C; lane 2, 23°C; lane 3, 4°C. Lane R; A + G chemical sequencing ladder. The 37°C DNase I footprint has been published previously (Chen & Helmann, 1995) and is included here for comparison.

$P_{hag}$ at 4, 23, and 37°C. The extent of DNase I protection of the non-template (nt) strand increases with temperature (Figure 1(a)). At 4°C, RNAP protects the DNA from −73 to near +1 with residual cleavages still detected at −52, −31, and −7 (Figure 1(a), lane 5). At 23°C, a region of partial protection extends further downstream to at least +9 and a DNase I hypersensitive site appears at −7 (lane 3). At 37°C protection extends to +21 (lane 1) and significant changes are observed in the −10 and −35 recognition regions: reactivity at −31 increases whle that at −7 decreases. Thus, structural distortions in the complex lead to enhanced DNase I cleavage predominantly in the −10 region at 23°C and in the −35 region at 37°C. Since these same regions are rendered DNase I sensitive by $\sigma^D$ protein even in the absence of the core subunits (Chen & Helmann, 1995), we suggest that these changes in the $E(\delta)\sigma^D$ complex are also due to $\sigma^D$ contacts. The DNase I footprint of $E(\delta)\sigma^D$ at $P_{hag}$ on the template (t) strand has been reported previously (Fredrick *et al.*, 1995) and extends from −70 downstream to at least +20. DNase I sensitive sites are observed with a ~10 bp periodicity in the upstream part of $P_{hag}$ (near −62, −52, −43, and −31) in both the 23°C and 37°C complexes, consistent with a predominant interaction along one face of the DNA helix (Ozoline & Tsyganov, 1995). Interesting temperature-dependent effects on DNase I sensitivity are also observed in the UP element. Protection of the UP element is observed throughout this temperature range, but cleavage at −43 and between −65 and −73 increases with temperature, suggesting that the interactions of α with DNA in this region may also be changing.

### DNA-melting as a function of temperature at $P_{hag}$

In parallel with the above DNase I footprinting studies, we measured the location and extent of promoter melting by $E(\delta)\sigma^D$. Permanganate oxidation of the pyrimidine 5,6 double bond is very slow in double-stranded, *B*-form DNA but quite rapid when the DNA is single-stranded or when the stacking of adjacent bases is disrupted (Sasse-Dwight & Gralla, 1991). In this study we have not distinguished between these two possibilities, but most of the reactivity we observe is in regions known to be single-stranded at other promoters, as judged by chemical modification of positions involved in hydrogen bonding with the complementary strand (Cowing *et al.*, 1989; Kirkegaard *et al.*, 1983; Siebenlist, 1979; Spassky *et al.*, 1985). Therefore, we will refer to regions of permanganate reactivity as single-stranded or melted, with the caveat that these may represent unstacked but still hydrogen-bonded base-pairs in some instances (Newlands *et al.*, 1991). Conversely, a lack of permanganate reactivity in single-stranded regions could result from protection of the thymine 5,6 double bond by protein contacts or by an unfavorable local electrostatic environment.

At 37°C, thymine residues at −4, −7, and −8 (nt) are highly reactive to permanganate with weaker reactivity observed at −15, −10, −1, and +2 (nt) (Figure 1(b)). The weak reactivity at −15 and +2 (nt) at 4°C is not dependent on RNAP (see below). Interestingly, the −4, −7, and −8 reactivity is almost fully established by 23°C. In contrast, the 4°C complex displays reactivity at −10 (nt) but not at the more start site proximal positions.

The experiments presented in Figure 1 demonstrate that $E(\delta)\sigma^D$ RNAP binds $P_{hag}$ at 4°C and induces a distortion near −10. As the temperature is increased, DNA-melting appears to propagate downstream in a uni-directional manner (Figure 1(b)). We next analyzed DNA-melting at $P_{hag}$ in the presence and absence of δ, a RNAP subunit known to affect DNA-melting (Achberger *et al.*, 1982; Juang & Helmann, 1994a, 1995). For these studies, we used a preparation of *B. subtilis* core lacking δ (Juang & Helmann, 1994a) and reconstituted RNAP by addition of $\sigma^D$ and δ purified from *E. coli* overproducing strains (Chen & Helmann, 1995;

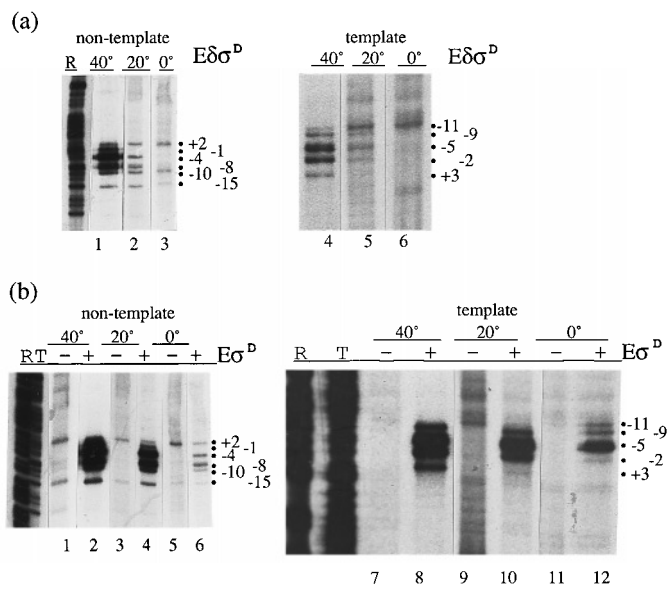



**Figure 2.** Potassium permanganate reactivity of $P_{hag}$ promoter DNA. Effects of temperature and δ factor on DNA-melting. (a) Potassium permanganate cleavage of $P_{hag}$ DNA in the presence of $E\delta\sigma^D$ holoenzyme on the non-template (nt) strand (lanes 1 to 3) and template (t) strand (lanes 4 to 6). Reactions contained reconstituted $E\sigma^D$ RNAP and a five-fold molar excess (over core) of δ incubated with DNA at the indicated temperature. (b) Potassium permanganate cleavage of $P_{hag}$ DNA (nt; lanes 1 to 6 and t; lanes 7 to 12). Reactions were performed at the indicated temperature and contained either $E\sigma^D$ RNAP (even lanes) or no added protein (odd lanes). Lane R: A and G chemical sequencing ladder. Lane T: T specific chemical sequencing ladder.

López de Saro *et al.*, 1995). Neither δ alone nor Eδ induce permanganate reactivity under these conditions (Juang & Helmann, 1994a).

RNAP reconstituted with a stoichiometric excess of δ, $E\delta\sigma^D$, induces permanganate reactivity at several position on both the non-template (nt) and template (t) strands of $P_{hag}$ (Figure 2(a)). The $E\delta\sigma^D$ 0°C complex induces reactivity at −10 (nt) and −11 (t), but not at −9 (t) (Figure 2(a), lanes 3 and 6). Neither the −10 (nt) nor the −11 (t) reactivity is detected in the absence of protein (e.g. Figure 2(b), odd numbered lanes). Therefore, $E\delta\sigma^D$ induces a distortion apparently localized to the CCGATAT portion of the −10 element (−11 and −10 positions underlined). This nucleated intermediate ($RP_n$) is observed reproducibly and is also the major species present at 10°C (data not shown).

At 20°C, $E\delta\sigma^D$ induces reactivity at −10, −8, −7 and −4 (nt) and at −11, −9, −6, −5 (t) (Figure 2(a), lanes 2 and 5). Under these conditions, −11 reactivity is stronger than −5 (t); the opposite of what is observed in the 40°C complex (lane 4). These 20°C complexes define a partially melted intermediate (characterized by reactivity between −11 and −4) which we assign as $RP_{-4}$. At 40°C, the −1 (nt) and −2 and +3 (t) positions become reactive suggesting that at least some of the binary complexes have progressed to a fully melted state ($RP_{+3}$).

DNA-melting proceeds through a similar series of intermediates in the absence of δ (Figure 2(b)). At 0°C (and 10°C, data not shown), $E\sigma^D$ establishes a partially opened complex ($RP_{-4}$) with reactivity localized primarily between −4 and −10 (nt) and between −5 and −11 (t) (lanes 6 and 12). With the exception of −5 (t), reactivity is weak compared to higher temperatures suggesting that the DNA is only partially melted in $RP_{-4}$ or that there is a mixture of $RP_{-4}$ and unreactive (closed) complexes under these conditions. At 20°C, $E\sigma^D$ extends the transcription bubble to include −2 (t) and (weakly) −1 (nt) (lanes 4 and 10), but not as far as +2 (nt) or +3 (t). We assign this complex as $RP_{-1}$. Reactivity at −11 (nt) is greatly decreased by the $RP_{-4}$ to $RP_{-1}$ transition. Finally, at 40°C, a fully extended transcription bubble, assigned as $RP_{+3}$, is visualized with reactivity extending from −10 (nt) to +3 (t) (lanes 2 and 8). Since the −11 (t) position is not reactive in these complexes, the probable upstream limit of DNA-melting is near −10. Although reactivity is observed at −15 (nt) this position is also reactive in naked DNA (lane 1).

Based on these observations, we define four intermediates at $P_{hag}$: $RP_n$ (reactivity limited to −11 and −10), $RP_{-4}$ (−11 to −4), $RP_{-1}$ (−10 to −1) and $RP_{+3}$ (−10 to +3). These complexes are observed reproducibly and appear to define distinct intermediates although, in some conditions, the experimentally observed permanganate reactivity is best explained as an equilibrium mixture of two or more of these complexes.

## δ alters DNA-melting in pre-formed RNAP-promoter complexes

Clearly, $E\sigma^D$ and $E\delta\sigma^D$ do not form equivalent complexes under otherwise identical conditions. Next, we tested whether δ could alter pre-formed $E\sigma^D$-$P_{hag}$ complexes (Figure 3). We added δ to $E\sigma^D$-$P_{hag}$ complexes at 20°C, a temperature which allows significant strand separation for $E\sigma^D$, but not for the $E\delta\sigma^D$ (Figure 2). After δ addition, the RNAP-promoter complex changed gradually into a more closed form, as judged by decreased permanganate reactivity at −11, −9, −6, −5, −2, and

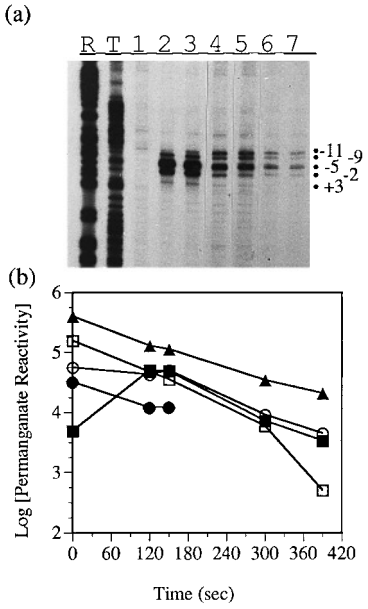



**Figure 3.** Effect of δ on open complexes at 20°C. (a) Potassium permanganate cleavage of $P_{hag}$ DNA (t). Lane 1, no protein control; lane 2, $E\sigma^D$ holoenzyme; lanes 3 to 7, $E\sigma^D$ holoenzyme after incubation with purified δ factor for 0, 120, 150, 300, 390 seconds, respectively. Lane T, thymine specific chemical sequencing ladder. Lane R, A and G chemical sequencing ladder. (b) Graphical representation of $P_{hag}$ melting *versus* time after δ addition. The intensity of the bands corresponding to thymine residues at −11 (■), −9 (○), −5/−6(▲), −2 (□) and +3 (●) were measured by phosphorimaging. Note that the signals corresponding to T −5 and T −6 were combined for this analysis.

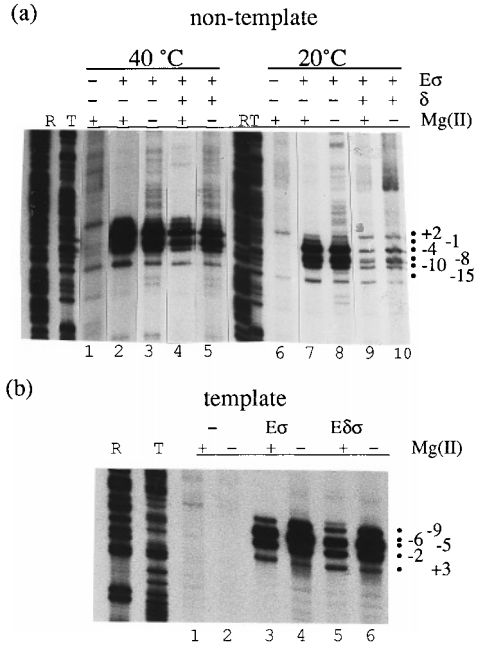



**Figure 4.** Effects of Mg(II) and δ on open complex formation at $P_{hag}$. Binary complexes were formed between $\sigma^D$ RNAP and $P_{hag}$ DNA. (a) Reactivity (nt) at 40°C (lanes 1 to 5) or 20°C (lanes 6 to 10) with either $E\sigma^D$ (lanes 2, 3, 7 and 8) or $E\delta\sigma^D$. $Mg^{2+}$ was at 6.4 mM but was chelated by an excess of EDTA in the minus $Mg^{2+}$ lanes (see Materials and Methods; for comparison, all the preceding footprinting experiments were performed in the presence of 0.5 mM $Mg^{2+}$). (b) Reactivity (t) at 40°C in the presence of no RNAP (lanes 1 and 2), $E\sigma^D$ (lanes 3 and 4), or $E\delta\sigma^D$ (lanes 5 and 6) in the presence and absence of available $Mg^{2+}$.

+3 (t) (Figure 3(a)). Reactivity near the center of the transcription bubble (−5, −6, −2 (t)) decreases as a simple exponential decay with a half-time of ca. 90 seconds (Figure 3(b)). Close inspection of the permanganate reactivity, however, reveals an intermediate in this process: the initial $E\sigma^D$ and the final $E\delta\sigma^D$ complexes display low reactivity at −11 (t) while at 120 and 150 seconds after δ addition (Figure 3(a), lanes 4 and 5) a complex is present with enhanced reactivity at −11 (t). We postulate that this represents a transient accumulation of either $RP_{-4}$ or $RP_n$ or both. The complexes present at the last four time points are all characterized by permangate reactivity at $-5 > -11 > -9 \approx -2$ while the starting complex is characterized by $-5 > -2 > -9 \gg -11$. Therefore δ induces a transition from the $RP_{-1}$ complex formed by $E\sigma^D$ to the mixture of $RP_{-4}$ and $RP_n$ formed by $E\delta\sigma^D$ with a half-time of about 90 seconds. Between two and five minutes after δ addition the level of permanganate reactivity decreases but the pattern does not change as judged from long exposures of the later time points (data not shown). Thus, there appears to be a time-dependent accumulation of unreactive complexes or displacement of RNAP from the promoter under these conditions

## Effects of δ and $Mg^{2+}$ on open complex formation

As reported previously for both *E. coli* RNAP at λ $P_R$ (Suh *et al.*, 1993) and *Thermotoga maritima* RNAP at T7 $A_1$ (Meier *et al.*, 1995), $Mg^{2+}$ increases the ability of $\sigma^D$ RNAP to melt the start site of transcription. The 40°C complexes of $E\sigma^D$ and $E\delta\sigma^D$ at $P_{hag}$ display permanganate reactivity between −11 and +3 and, in each case, $Mg^{2+}$ increases the reactivity at −1 (nt) (Figure 4(a)) and +3 (t) (Figure 4(b)). Thus, $Mg^{2+}$ favors the $RP_{-1}$ to $RP_{+3}$ transition. On the template strand, $Mg^{2+}$ decreases reactivity at more upstream positions, possibly due to increased association of the template with the active site region of RNAP (Figure 4(b), lanes 3 *versus* 4 and 5 *versus* 6). At 20°C, $Mg^{2+}$ leads to increased reactivity at −1 (nt) for $E\sigma^D$, but not for $E\delta\sigma^D$ (Figure 4(a), lanes 7 to 10). Hence, $Mg^{2+}$ alone is not able to overcome the anti-melting effect of δ, consistent with the fact that the experiments of Figure 2 contained $Mg^{2+}$.

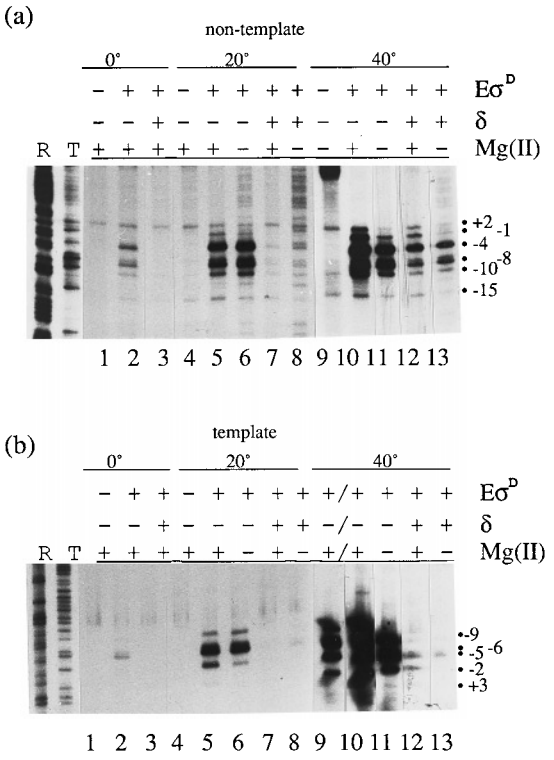



**Figure 5.** Effects of $Mg^{2+}$ and δ on open complex formation at $P_{hag}$(−UP). Potassium permanganate footprinting of (a) non-template and (b) template strands of $P_{hag}$(−UP). Reactions contained the indicated proteins and were incubated at the indicated temperature. In part (b), lanes 10 to 13 are from an autoradiograph exposed three-fold longer than lanes 1 to 9 (lanes 9 and 10 are the same lane). Lane T, thymine specific chemical sequencing ladder. Lane R, A + G chemical sequencing ladder.

The effects of δ and $Mg^{2+}$ on DNA-melting are even more apparent in studies performed using a derivative of $P_{hag}$ [$P_{hag}$(−UP)] in which DNA sequences upstream of −41 have been replaced by vector DNA (Figure 5). As noted with $P_{hag}$, $E\sigma^D$ induces a low level of permanganate reactivity at $P_{hag}$(−UP) even at 0°C, indicative of some formatio of $RP_{-4}$ (Figure 5, lanes 2). At 20°C, $E\sigma^D$ forms $RP_{-1}$ (lanes 5 and 6) while at 40°C strand separation appears to be complete ($RP_{+3}$). Reactivity at both the −2 and +3 (t) and −1 (nt) is strongly stimulated by $Mg^{2+}$, indicating that $Mg^{2+}$ stabilizes both $RP_{-1}$ and $RP_{+3}$ relative to $RP_{-4}$.

In contrast with $E\sigma^D$, $E\delta\sigma^D$ induces much less permanganate reactivity under most conditions. The lack of permanganate reactivity at 20°C suggests that $E\delta\sigma^D$ interacts weakly with $P_{hag}$(−UP) under these conditions, consistent with DNase I protection (data not shown) and electrophoretic mobility shift assays (Fredrick *et al.*, 1995). Even at 40°C, the intensity of the permanganate reactivity is substantially reduced by δ (Figure 5(a)) or not visible except in long exposures (Figure 5(b), lane 12). Thus,

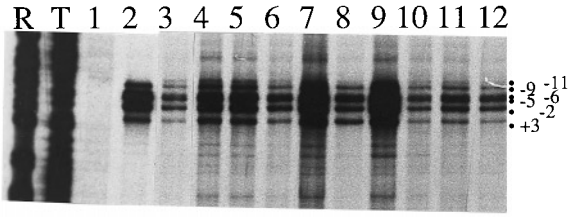



**Figure 6.** Effects of nucleotides on $P_{hag}$ DNA-melting at 40°C. Potassium permanganate cleavage of $P_{hag}$ DNA (t) at 40°C. Lane 1, no protein control. Lane 2, $E\sigma^D$ RNAP. Lane 3, $E\delta\sigma^D$ RNAP. Lanes 4 to 12, $E\delta\sigma^D$ RNAP in the presence of: lane 4, GTP; lane 5, ATP; lane 6, GDP; lane 7, GMP; lane 8, GTP + UTP; lane 8, GTP + UTP + ATP; lane 9, GTP + UTP + ATP + heparin; lane 10 GpU; lane 11, GpU + ATP. All nucleotides were added to a final concentration of 0.3 mM.

in the absence of the stabilizing influence of the α-UP element interaction, δ prevents the quantitative formation of mature open complexes ($RP_{+3}$) at $P_{hag}$.

## Effects of NTPs on open complex formation

We next tested whether NTPs could alter the extent or location of strand separation at $P_{hag}$. Significantly, addition of either GTP or ATP, but not CTP or UTP (data not shown), was able to overcome the inhibition of promoter-melting by δ (Figure 6, lanes 2 to 5). In contrast, nucleotide addition had little if any effect on template strand reactivity induced by $E\sigma^D$ RNAP at 40°C, suggesting that the DNA was already fully melted under these con-

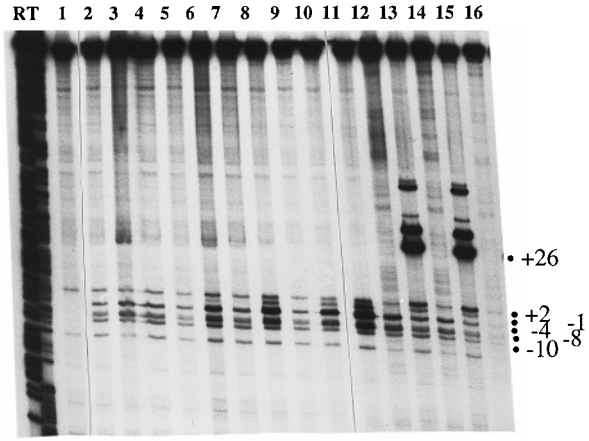



**Figure 7.** Effects of nucleotides on $P_{hag}$ DNA-melting at 20°C. Potassium permanganate cleavage of $E\delta\sigma^D$ complexes on $P_{hag}$ DNA (nt) at 20°C. Lane 1, no protein control; lane 2 $E\sigma^D\delta$ with no added nucleotide; lane 3, $E\sigma^D\delta$ + EDTA; lane 4, GTP; lane 5, GDP; lane 6, GMP; lane 7, UTP; lane 8, GTP + UTP; lane 9 GpU; lane 10, GpU + ATP; lane 11, GTP + UTP + ATP; lane 12, GTP + UTP + ATP + EDTA; lane 13, GpU + GTP + ATP + CTP; lane 14, GpU + GTP + ATP + CTP + EDTA; lane 15, GpU + GTP + ATP + CTP + heparin; lane 16, GpU + GTP + ATP + CTP + heparin + EDTA.

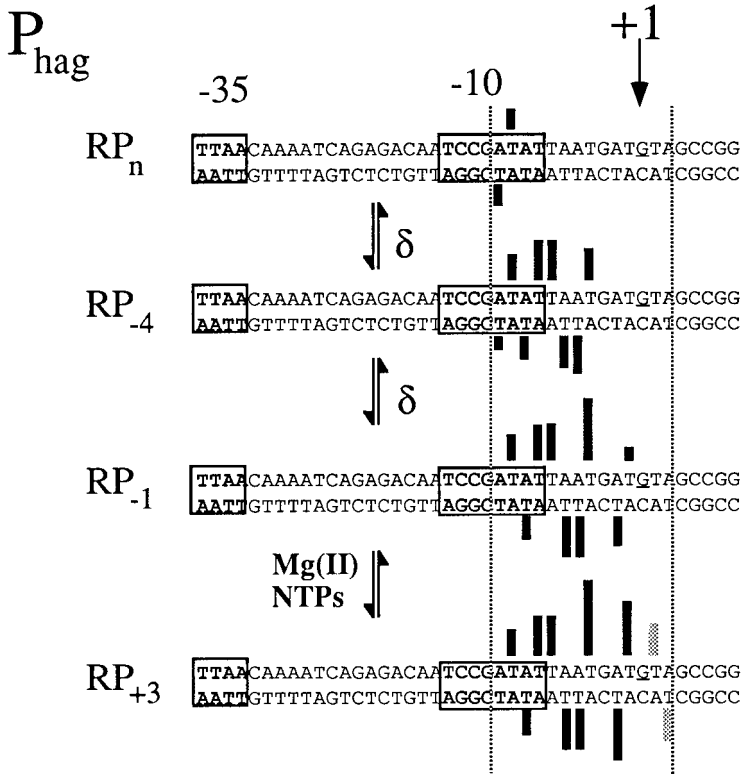



**Figure 8.** Model for promoter melting at $P_{hag}$. The patterns of permanganate reactivity in different complexes formed at $P_{hag}$ and the principle steps affected by $Mg^{2+}$, NTPs, and δ are summarized. The −35 and −10 elements are boxed and vertical dotted lines define the observed boundaries of the transcription bubble. The heights of the bars correspond to the relative intensity of the permanganate signals at the indicated position. Stripping indicates signals which are strongly stimulated by $Mg^{2+}$.

ditions (lane 2 and data not shown). These NTP effects were dependent on $Mg^{2+}$ (data not shown) and suggest that binding of a purine to RNAP stabilizes the open conformation in the vicinity of the transcription start site. Since the non-template sequence near the start of transcription is 5′-ATGTAGC (start site underlined), neither ATP nor GTP alone should allow nucleotide polymerization. Indeed, GMP alone is also highly effective at inducing start site melting (Figure 6, lane 7) and leads to greater reactivity than GTP (lane 5), GDP (lane 6), the first two substrates (GTP and UTP; lane 8), or the initiating dinucleotide GpU (lane 11). Overall, the greatest permanganate reactivity was induced by either GMP or a combination of substrates (G, U, and A) sufficient for synthesis of products up to the tetramer (lane 9). The observation that GMP is more effective than GTP in inducing permanganate reactivity may simply reflect an increased equilibrium level of fully melted ($RP_{+3}$) complex. We cannot rule out, however, a possible inhibitory role of the negatively charged β and γ phosphate groups in GTP on attack of the DNA by permanganate ion.

Similar nucleotide effects are apparent when non-template strand reactivity is measured at 20°C (Figure 7). Melting near the start site (−1 and +2; nt) is dramatically increased by GMP (lane 6) or by combinations of substrates able to support bond formation: G and U (lane 8), GpU and A (lane 10), or G, U, and A (lane 11). This suggests that binding of GMP or chain initiation shifts the equilibrium distribution of binary complexes from $RP_{-4}$ to the more fully melted $RP_{-1}$, $RP_{+3}$ and subsequent initial transcribing complexes. In contrast, neither the initiating dinucleotide, GpU, nor GDP are able to increase DNA-melting under these conditions. Note that since +2 (nt) is somewhat reactive in the absence of protein (lane 1), this thymine is a less reliable indicator of strand separation than −1 (nt).

Finally, we demonstrate that upon addition of GpU, A, G, and C the majority of the RNAP complexes advance along the DNA template (a combination of substrates sufficient for formation of a stable elongation complex paused at position +25 due to the absence of the UTP templated at position +26). The strong reactivity noted near +26 presumably corresponds to RNAP paused at position +25 while the downstream signals are likely to arise from read-through to subsequent positions requiring UTP. The downstream reactivity varies between experiments and may be due to contamination with UTP (which can arise from spontaneous deamination of CTP). As expected, chain elongation requires $Mg^{2+}$ and the resulting elongation complexes are heparin-stable (lanes 13 to 15). These data demonstrate that the majority of the binary complexes are active and competent for chain elongation.

## Discussion

Our analysis of promoter activation at $P_{hag}$ suggests the formation of (1) a nucleated intermediate, $RP_n$, with a distortion near the −11/ −10

base step, (2) an initial open complex, $RP_{-4}$, (3) an intermediate complex, $RP_{-1}$, and (4) a fully melted open complex, $RP_{+3}$ (Figure 8). These complexes are distinct in patterns of permanganate reactivity and are observed reproducibly suggesting that they represent discrete intermediates. Similar partially melted intermediates are also observed at two other $\sigma^D$-dependent promoters, $P_{fliD}$ and $P_{flgM}$ (data not shown). A common assumption in these and related studies is that the binary complexes formed at different temperatures resemble the transient intermediates which form during initiation at a single temperature (Buckle & Buc, 1994). This assumption, however, has not been explicitly tested in this work.

### Phosphate backbone contacts at $P_{hag}$

The backbone contacts made by $E(\delta)\sigma^D$ RNAP at $P_{hag}$ change in a temperature-dependent fashion (Figure 1) and correlate with the extent of DNA-melting. The downstream boundary of the DNase I footprint extends from near +1 (at 4°C) to +9 (23°C) and finally to +20 (37°C). Note that the −31 (nt) DNase I sensitive site increases with temperature while the hypersensitive site at −7 (nt) site is most pronounced in the 23°C complex. This result is inconsistent with a single-step conversion of a closed complex to a fully melted open complex and suggests the presence of additional intermediates. In the upstream region, protection is face of the helix dependent and includes the UP element (Fredrick *et al.*, 1995). Interestingly, protection of the UP element is strongest at low temperature, suggesting that these contacts may weaken during the process of promoter melting.

The DNase I footprint of the 4°C $E(\delta)\sigma^D$-$P_{hag}$ complex resembles closed complexes formed by *E. coli* $E\sigma^{70}$ and $E\sigma^{32}$ (Kovacic, 1987; Mecsas *et al.*, 1991) and *B. subtilis* $E\sigma^A$ (Juang & Helmann, 1994a,b, 1995). However, some DNA-melting (or distortion) is detected at −10 (nt) under these conditions (Figures 1(b) and 2(a)). By 23°C, the region of DNA backbone protection extends to about +9, with a notable hypersensitive site at −7, and DNA-melting extends from −10 to −1 ($RP_{-1}$). Similar DNase I footprints, with downstream boundaries between +5 and +10, were reported for the 37°C $E\sigma^A$ RNAP complexes at the *tms*, *citB* and ϕ29 G3b promoters while, under identical conditions, *E. coli* RNAP forms complexes extending downstream to near +20 (Whipple & Sonenshein, 1992; Chang *et al.*, 1992). RNAP also displays a shortened footprint at $P_{trnS}$ at 20°C (Juang & Helmann, 1995). Finally, at 37°C a fully melted complex is formed with DNase I protection extending to +21, characteristic of open complexes formed by *E. coli* RNAP (Ozoline & Tsyganov, 1995). Our data suggest that the variability in DNase I footprints reported for $E\sigma^A$ complexes may reflect differences in the extent of promoter melting.

### Nucleation of promoter-melting at $P_{hag}$

The mechanisms used by bacterial RNAP to form and stabilize the transcription bubble are not well understood (deHaseth & Helmann, 1995). At many well studied *E. coli* promoters the transcription bubble forms in a concerted mnner with a simultaneous increase in base reactivity to single-strand selective probes over a narrow temperature range (Cowing *et al.*, 1989; Kirkegaard *et al.*, 1983; Spassky *et al.*, 1985). This highly cooperative melting transition suggests that nucleation is slow relative to the subsequent expansion of the transcription bubble, but does not preclude a role for the TATA element in nucleating strand separation. Indeed, in some cases melting may be a gradual rather than a cooperative process. Temperature-dependent analysis of melting at several *E. coli* promoters supports a mechanism in which melting nucleates near −10: examples include several variants of *gal*P1 (Burns & Minchin, 1994; Grimes *et al.*, 1991), binary complexes of the $\sigma^N$ holoenzyme (Morris *et al.*, 1994), and melting of the T7 A1 promoter by *Thermotoga maritima* RNAP (Meier *et al.*, 1995). Similarly, $E\sigma^A$ can form partially melted intermediates during melting at $P_{trnS}$ (Juang & Helmann, 1995). The ability to observe several intermediate states in melting at $P_{hag}$ may be fortuitous: other promoters may pass through similar intermediates, may melt from the center of the transcription bubble outward, or may melt in a highly cooperative fashion.

Several lines of evidence point to a key role for the TATA element, conserved in both bacterial and eukaryotic promoters, in favoring pre-melting transitions in the promoter DNA (Travers, 1987). Theoretical calculations identify a characteristic peak of DNA instability near the −10 element, due largely to the low stacking energy of the TA and AT dinucleotides (Margalit *et al.*, 1988). Negative supercoiling induces structural transitions at $P_{tyr}$ detectable by $S_1$ nuclease mapping (Drew *et al.*, 1985). Similary, copper orthophenanthroline footprinting identifies highly reactive sites in the −10 regions of several *lac* and *gal* promoter variants (Spassky *et al.*, 1988) while DNA-bending induces permanganate reactivity within the −10 element at *E. coli ilv* $P_G$ (Parekh & Hatfield, 1996). Structural distortions introduced into the TATA element, such as oxidation of thymine by osmium tetroxide (Chan *et al.*, 1989), abasic sites (Werel *et al.*, 1991), or base-pair mismatches (Roberts & Roberts, 1996) can also increase rates of RNAP binding and initiation. These data are all consistent with a role for the TATA element in creating a locus of initial DNA-melting which can then be stabilized and propagated downstream by interactions between single-stranded DNA and RNAP.

We propose that the alternating AT base pairs in the $\sigma^D$ −10 consensus, GCCGATAT, serve as a similar nucleation site for strand separation. Melting appears to nucleate within the −10 element at a specific AT base step, either by a localized kink-

ing of the DNA or perhaps a ''base-flipping'' mechanism. Indeed, the upstream AT base step is invariant in $\sigma^D$-dependent promoters and a variant promoter lacking this AT step is inactive *in vitro* (K. Fredrick & J.D.H. unpublished results). A similar melting pathway has been proposed for $E\sigma^N$ which, like $E\sigma^D$, distorts an AT bp just downstream of a GC-rich element (Morris *et al.*, 1994). Although we consistently detect a nucleated intermediate at $P_{hag}$, we have not detected an analogous intermediate at $P_{hag}$(−UP), $P_{fliD}$, or $P_{flgM}$, suggesting that this complex, if formed, is unstable relative to other partially melted intermediates (data not shown).

### δ, $Mg^{2+}$, and substrates all affect promoter melting by $\sigma^D$ RNAP

We have used δ protein, $Mg^{2+}$, and nucleoside substrates, in various combinations, to alter the equilibrium distribution of RNAP complexes at $P_{hag}$. The δ subunit affects the ability of RNAP to melt promoter DNA: $E\delta\sigma^A$ forms closed complexes at $P_{ilv}$ even at 40°C whereas $E\sigma^A$ forms an open complex (Juang & Helmann, 1994a). In contrast, both $E\sigma^A$ and $E\delta\sigma^A$ are able to form open complexes at the stronger *trnS* promoter, but the transition temperature (point of half-maximal melting) is increased by at least 15°C by δ (Juang & Helmann, 1995). We now find that δ also alters the promoter interactions of $\sigma^D$ RNAP by opposing the full maturation of the binary complex. Despite its profoud effects on promoter interactions and RNAP activity, the biological role of δ remains a mystery. Mutants lacking δ are viable and are not grossly defective in growth or sporulation (Lampe *et al.*, 1988).

We do not yet understand the mechanisms by which δ exerts its anti-melting effect. However, it is clear that RNAP can exist in multiple conformations influenced by both σ and nascent RNA (Polyakov *et al.*, 1995). Significantly, binding of polyanions such as heparin can displace RNAP from DNA by interaction in the RNA-binding site rather than by direct competition for the template site (cf. Aiyar *et al.*, 1994). We postulate that δ, which interacts with the RNA-binding site through a polyanionic carboxyl-terminal region (López de Saro *et al.*, 1995), acts as an allosteric effector of RNAP conformation and thereby opposes the conformational changes accompanying promoter melting.

$Mg^{2+}$ also has a profound influence on the nature and extent of strand separation. A structural role for $Mg^{2+}$ in promoter activation was first inferred from the observation that the rate of open complex dissociation at λ $P_R$ is very sensitive to added NaCl ($d \log k_d / d \log[Na^+] = 7.7$) but not to added $MgCl_2$($d \log k_d / d \log[Mg^{2+}] = 0.4$) (Suh *et al.*, 1992). This difference predicts the existence of an initial open complex, $RP_{01}$ (perhaps similar to $RP_{-1}$ in this paper), in which eight $Na^+$ ions are displaced (or four $Mg^{2+}$) followed by a $Mg^{2+}$-dependent isomerization to a second open complex, $RP_{02}$, in which three $Mg^{2+}$ are bound (Suh *et al.*, 1992). Footprinting studies indeed reveal a $Mg^{2+}$-dependent increase in DNA-melting near the edges of the transcription bubble (Suh *et al.*, 1993; Craig *et al.*, 1995). Our results with $P_{hag}$ support the idea that $Mg^{2+}$ may play a general role in the late stages of start site opening, but also identify additional early intermediates in this process.

The ability of substrates to affect the degree of strand separation is well established. RNAP has two biochemically distinct binding sites for NTP substrates: an initiation site and an elongation site (Wu & Goldthwait, 1969a,b). The *de novo* synthesis of RNA begins when both NTP sites are occupied by bases specified by the template strand of the promoter. The initiation site preferentially binds purines and can also bind NDPs and NMPs while the elongation site requires NTPs (Kumar, 1981). At $P_{hag}$, substrates increase DNA-melting, particularly near the transcription start site. While the stabilization and expansion of the $P_{hag}$ transcription bubble under conditions allowing transcript initiation is similar to that reported at other promoters (Dobinson & Spiegelman, 1987; Newlands *et al.*, 1991; Rojo *et al.*, 1993), the ability of a single NMP to increase DNA-melting has not, to our knowledge, been observed previously. The effects we observe are most consistent with interactions at the initiating NTP site: either ATP or GTP increase melting and, of the nucleotides tested, GMP appears to have the strongest effect.

### A model for promoter activation

A recent convergence of biophysical, biochemical and genetic investigations has led to detailed structural models for both initiating (deHaseth & Helmann, 1995; Roberts & Roberts, 1996) and elongating (Nudler *et al.*, 1996; Chan & Landick, 1994; Chamberlin, 1995) RNAP-DNA complexes. Within the context of these models, we can speculate about possible interactions contributing to the formation of the intermediates we observe. Promoter recognition is mediated by contacts of σ with the −35 and −10 elements (Dombroski *et al.*, 1992; Gross *et al.*, 1992; Helmann, 1994), contacts between α and the upstream promoter region (Fredrick *et al.*, 1995; Gaal *et al.*, 1996; Ross *et al.*, 1993), and non-specific interactions of β and β′ with DNA. In the closed complex, DNA may wrap around RNAP leading to a localized destabilization of the −10 element in a region of alternating AT base-pairs (Travers, 1987). Promoter melting then nucleates when the non-template strand establishes stabilizing interactions with the proposed ''melting motif'' in σ region 2.3 (Juang & Helmann, 1994; deHaseth & Helmann, 1995; Rong & Helmann, 1994). Structural analyses of a $\sigma^{70}$ fragment confirm that the functionally important aromatic amino acids in region 2.3 are appropriately arrayed to form a single-strand DNA binding surface (Malhotra *et al.*, 1996). Importantly, holoenzyme

binds tightly and selectively to oligonucleotides containing the −10 non-template consensus in a reaction apparently mediated by σ region 2 (Severinova *et al.*, 1996). As predicted, this binding is single-strand selective and is affected by $\sigma^A$ region 2.3 mutations which impair promoter melting (X. Huang & J.D.H., unpublished results).

Further expansion of the transcription bubble is proposed to reflect association of the template strand with the active site. Elongation complexes are stabilized by two biochemically distinct interactions at the rear (R) and front (F) of the complex (Nudler *et al.*, 1996), and it seems reasonable to propose that these same interactions may contribute, in part, to the stability of the initiation complex. The F site is duplex specific and binds just ahead of the active site (Nudler *et al.*, 1996). This interaction, mediated by a zinc finger domain in the amino terminus of β′, may account for the downstream progression of the DNA contacts noted during the development of open complexes. The R site binds six nucleotides of the single-stranded template DNA immediately upstream of the active site and may contribute to the unidirectional expansion of the transcription bubble. Intriguingly, the same region of RNAP responsible for the R interaction, the carboxyl-terminal domain of β, binds to the initiating NTP (Severinov, *et al.*, 1995). Thus, a conformational change elicited by binding of an NTP (or NMP in our experiments) might help establish the R site interaction and thereby effect the $RP_{-1}$ to $RP_{+3}$ transition. RNAP binds both $Mg^{2+}$, in the elongating BTP site, and $Zn^{2+}$, in the initiating NTP site, as essential cofactors for NTP polymerization (Beal *et al.*, 1990). Although the $Mg^{2+}$ binding site in β′ is not absolutely required for promoter opening (Zaychikov *et al.*, 1996), this site may nevertheless contribute to the downstream expansion of the transcription bubble.

## Materials and Methods

### Isolation and labeling of promoter fragments

For the experiments shown in Figure 1, DNA fragments containing $P_{hag}$ were purified from pYFC-16 (Chen & Helmann, 1995) by digestion with either *Bsp*120i or *Eag*I, depending on the strand to be labeled. The DNA was then treated with calf-intestine alkaline phosphatase (New England Biolabs), 5′ end-labeled with [γ-$^{32}$P]ATP and phage T4 polynucleotide kinase, and the promoter containing fragment (267 bp) removed by digestion with the second enzyme (either *Bsp*120i or *Eag*I) and purified by 5% PAGE and elution using 0.5 M ammonium acetate, 10 mM magnesium acetate, and 1 mM EDTA. Fragments labeled at the *Bsp*120i 5′-end are labeled on the template strand. For all subsequent experiments, $P_{hag}$ was prepared as a 334 bp polymerase chain reaction (PCR) fragment using one 5′ end-labeled and one unlabeled primer (5′-TAAAGGGAACAAAAGCTGGGTACCG-3′ and 5′-TACGACTCACTATAGGGCGAATTGG-3′) for the template and non-template strand, respectively). Oligonucleotides were 5′-end-labeled using phage T4 polynucleotide kinase as described (Chen & Helmann, 1995) before the PCR reaction and products were recovered using a PCR product purification kit (Promega).

The DNA fragment containing $P_{hag}$(−UP) was excised from pHAG-41 (Fredrick *et al.*, 1995) as a 104 bp *Eco*RI to *Bam*HI fragment and cloned into pBKSII$^+$ (Stratagene) to generate pKF4K. For the experiment shown in Figure 5, the $P_{hag}$(−UP) containing DNA fragment was prepared using the PCR and one 5′ end-labeled and one unlabeled primer followed by purification of the product as above. The primers used were: 5′-TAAAGGGAACAAAAGCTGGGTACCG-3′ (nt, non-template strand) and 5′-TACGACTCACTATAGGGCG-AATTGG-3′ (t, template) with pKF4K as template.

### Purification of E, E(δ), δ, and $\sigma^D$

RNAP core enzyme containing near stoichiometric amounts of δ protein (E(δ)) was purified using FPLC MonoS chromatography as a final step as described previously (Chen & Helmann, 1995) and supplemented with a molar excess of $\sigma^D$ to generate E(δ)$\sigma^D$. For subsequent experiments, core was purified using BioRex-70 chromatography as described (Juang & Helmann, 1994a) and lacked detectable δ. This core was incubated with a molar excess of purified $\sigma^D$ at room temperature for ten minutes and the resulting E$\sigma^D$ holoenzyme was separated from free $\sigma^D$ by FPLC Superdex 200 (25 ml) chromatography in 50 mM Tris-HCl (pH 8.0), 0.1 mM EDTA, 1 mM DTT, 10% (v/v) glycerol, and 0.5 M NaCl. The resulting holoenzyme was dialyzed into 50 mM Tris-HCl (pH 8.0), 0.1 mM EDTA, 1 mM DTT, 50% (v/v) glycerol, and 50 mM NaCl for storage at −20°C. This enzyme was more stable during prolonged storage than core lacking $\sigma^D$. The $\sigma^D$ and δ proteins were purified from *E. coli* overproducing strains as described (Chen & Helmann, 1995; López de Saro *et al.*, 1995). When indicated, E$\sigma^D$ was supplemented with a five-fold stoichiometric excess of δ.

### DNase I footprinting

For the experiments of Figure 1(a), 0.3 pmol of labeled DNA fragment was incubated with 0.9 pmol E(δ) core and 6 pmol $\sigma^D$ in 25 μl binding buffer (40 mM Tris-HCl (pH 8.0), 0.5 mM $MgCl_2$, 50 mM NaCl, 1 mM DTT, 20% (v/v) glycerol, and 0.25 mg/ml BSA (bovine serum albumin) for ten minutes prior to incubation for one minute with RQ1 RNase I (ProMega) at a final concentration of 0.125 unit/μl (37 or 40°C), 0.25 unit/μl (23°C) or 1 unit/μl (4°C).

### Potassium permanganate footprinting

Potassium permanganate footprinting reactions in Figure 1 were done under the same conditions as the corresponding DNase I reactions using 0.3 pmol of DNA and procedures described previously (Juang & Helmann, 1994a,b). The binding buffer (25 μl) contained 0.5 mM $Mg^{2+}$, 7 μg/ml plasmid DNA (lacking a $\sigma^D$ promoter), and 0.24 mg/ml salmon testes DNA. 200 mM potassium permanganate was added for three minutes and reactions were terminated by addition of 200 μl permanganate stop solution (10 mM EDTA, 0.24 mg/ml sonicated salmon testes DNA, 1 M β-mercaptoethanol, 0.3 M solidum acetate, pH 7.0). Nucleic acids were recovered by ethanol precipitation and treated with 1 M piperidine as

described (Sambrook *et al.*, 1990) prior to heat denaturation and separation by 8 M urea/PAGE.

All subsequent potassium permanganate footprinting reactions containing 0.033 pmol DNA (PCR product), 1.67 pmol purified $E\sigma^D$ holoenzyme, and 9 pmol $\sigma^D$ incubated in 25 µl binding buffer (40 mM Tris-HCl (pH 8.0), 0.5 mM $MgCl_2$, 50 mM NaCl, 1 mM DTT, 20% (v/v) glycerol, 0.25 mg/ml BSA) for ten minutes at the indicated temperature prior to addition of 200 mM potassium permanganate (Sigma Chemical Co.) for three minutes. Reactions were processed as above. Quantification of specific T reactivity was determined using a Molecular Dynamics phosphorimaging system, with ImageQuant data analysis software.

## Acknowledgements

We thank Kurt Fredrick, Pieter deHaseth, and Rick Gourse for helpful discussions and Yue-Li Juang and Francisco López de Saro for gifts of core enzyme and δ protein. This work was supported by NIH grant GM-47446.

## References

Achberger, E. & Whiteley, H. R. (1981). The role of the δ peptide of the *Bacillus subtilis* RNA polymerase in promoter selection. *J. Biol. Chem.* **256**, 7424–7432.

Achberger, E., Hilton, M. D. & Whiteley, H. R. (1982). The effect of the delta subunit on the interaction of *Bacillus subtilis* RNA polymerase with bases in a SP82 early gene promoter. *Nucl. Acids Res.* **10**, 2893–2910.

Aiyar, S. E., Helmann, J. D. & deHaseth, P. L. (1994). A mismatch bubble in double-stranded DNA suffices to direct precise transcription initiation by *Escherichia coli* RNA polymerase. *J. Biol. Chem.* **269**, 13170–13184.

Arndt, K. M. & Chamberlin, M. J. (1990). RNA chain elongation by *Escherichia coli* RNA polymerase: factors affecting the stability of elongating ternary complexes. *J. Mol. Biol.* **213**, 79–108.

Beal, R. B., Pillai, R. P., Chuknyisky, P. P., Levy, A., Tarien, E. & Eichorn, G. L. (1990). Structural studies on the active site of *Escherichia coli* RNA polymerase. 2. Geometrical relationship of the interacting sites. *Biochemistry,* **29**, 5994–6002.

Buc, H. & McClure, W. R. (1985). Kinetics of open complex formation between *Escherichia coli* RNA polymerase and the *lacUV5* promoter: evidence for a sequential mechanism involving three steps. *Biochemistry,* **24**, 2712.

Buckle, M. & Buc, H. (1994). On the mechanism of promoter recognition by *E. coli* RNA polymerase. In *Transcription: Mechanisms and Regulation* (Conaway, R. C. & Conaway, J. W., eds), pp. 207–225, Raven Press, New York.

Buckle, M., Geiselmann, J., Kolb, A. & Buc, H. (1991). Protein-DNA cross-linking at the *lac* promoter. *Nucl. Acids Res.* **19**, 833–840.

Burns, H. & Minchin, S. (1994). Thermal energy requirement for strand separation during transcription initiation: the effect of supercoiling and extended protein DNA contacts. *Nucl. Acids Res.* **22**, 3840–3845.

Carpousis, A. J. & Gralla, J. D. (1980). Cycling of ribonucleic acid polymerase to produce oligonucleotides during initiation *in vitro* at the *lac* UV5 promoter. *Biochemistry,* **19**, 3245–3253.

Chamberlin, M. J. (1995). New models for the mechanism of transcription elongation and its regulation. *Harvey Lectures*, **88**, 1–21.

Chan, C. L. & Landick, R. (1994). New perspectives in RNA chain elongation and termination by *E. coli* RNA polymerase. In *Transcription: Mechanisms and Regulation*. 297–321, Raven Press, New York.

Chan, P. T., Sullivan, J. K. & Lebowitz, J. (1989). Site-directed chemical modification for probing DNA-protein interactions: osmium tetroxide modification of the −10 site of the *lac*UV5 promoter enhances open complex formation. *J. Biol. Chem.* **264**, 21277.

Chang, B. Y., Shyu, Y. T. & Doi, R. H. (1992). The interaction between *Bacillus subtilis* sigma-A ($\sigma^A$) factor and RNA polymerase with promoters. *Biochimie,* **74**, 601–612.

Chen, Y.-F. & Helmann, J. D. (1995). The *Bacillus subtilis* flagellar regulatory protein $\sigma^D$: overproduction, domain analysis, and DNA-binding. *J. Mol. Biol.* **249**, 743–753.

Cowing, D. W., Mecasa, J., Record, M. T., Jr & Gross, C. A. (1989). Intermediates in the formation of the open complex by RNA polymerase holoenzyme containing the sigma factor $\sigma^{32}$ at the *groE* promoter. *J. Mol. Biol.* **210**, 521–530.

Craig, M. L., Suh, W.-C. & Record, M. T., Jr (1995). $HO^{\cdot}$ and DNase I probing of $E\sigma^{70}$ RNA polymerase-λ $P_R$ promoter open complexes: $Mg^{2+}$ binding and its structural consequences at the transcription start site. *Biochemistry,* **34**, 15624–15632.

deHaseth, P. & Helmann, J. D. (1995). Open complex formation by *Escherichia coli* RNA polymerase: the mechanism of polymerase-induced strand separation of double helical DNA. *Mol. Microbiol.* **16**, 817–824.

Dobinson, K. F. & Spiegelman, G. B. (1987). Effect of the δ subunit of *Bacillus subtilis* RNA polymerase on initiation of RNA synthesis at two bacteriophage ϕ29 promoters. *Biochemistry,* **26**, 8206–8213.

Dombroski, A. J., Walter, W. A., Record, M. T., Jr, Siegele, D. A. & Gross, C. A. (1992). Polypeptides containing highly conserved regions of transcription initiation factor $\sigma^{70}$ exhibit specificity of binding to promoter DNA. *Cell,* **70**, 501–512.

Drew, H. R., Weeks, J. R. & Travers, A. A. (1985). Negative supercoiling induces spontaneous unwinding of a bacterial promoter. *EMBO J.* **4**, 1025–1032.

Fredrick, K., Caramori, T., Chen, Y. F., Galizzi, A. & Helmann, J. D. (1995). Promoter architecture in the flagellar regulon of *Bacillus subtilis*: high-level expression of flagellin by the $\sigma^D$ RNA polymerase requires an upstream promoter element. *Proc. Natl Acad. Sci. USA,* **92**, 2582–2586.

Gaal, T., Ross, W., Blatter, E. E., Tang, H., Jia, X., Krishnan, V. V., Assa-Munt, N., Ebright, R. H. & Gourse, R. L. (1996). DNA-binding determinants of the α subunit of RNA polymerase: novel DNA-binding domain architecture. *Genes Dev.* **10**, 16–26.

Grimes, E., Busby, S. & Minchin, S. (1991). Different thermal energy requirement for open complex formation by *Escherichia coli* RNA polymerase at two related promoters. *Nucl. Acids Res.* **19**, 6113–6118.

Gross, C. A., Lonetto, M. & Losick, R. (12992). Bacterial sigma factors. In *Transcriptional Regulation* (McKnight, S. L. & Yamamoto, K. R., eds),

pp. 129–176, Cold Spring Harbor Laboratory Press, Cold Spring Harbor, NY.
Helmann, J. D. (1991). Alternative sigma factors and the regulation of flagellar gene expression. *Mol. Microbiol.* **5**, 2875–2882.
Helmann, J. D. (1994). Bacterial sigma factors. In *Transcription: Mechanisms and Regulation* (Conaway, R. C. & Conaway, J. W., eds), pp. 1–17, Raven Press, New York.
Helmann, J. D. & Chamberlin, M. J. (1988). Structure and function of bacterial σ factors. *Annu. Rev. Biochem.* **57**, 839–872.
Hilton, M. D. & Whiteley, H. R. (1985). UV cross-linking of the *Bacillus subtilis* RNA polymerase to DNA in promoter and nonpromoter complexes. *J. Biol. Chem.* **260**, 8121–8127.
Juang, Y.-L. & Helmann, J. D. (1994a). The δ subunit of *Bacillus subtilis* RNA polymerase: an allosteric effector of the initiation and core-recycling phases of transcription. *J. Mol. Biol.* **239**, 1–14.
Juang, Y.-L. & Helmann, J. D. (1994b). A promoter melting region in the primary σ factor of *Bacillus subtilis*: identification of functionally important aromatic amino acids. *J. Mol. Biol.* **235**, 1470–1488.
Juang, Y.-L. & Helmann, J. D. (1995). Pathway of promoter melting by *Bacillus subtilis* RNA polymerase at a stable RNA promoter: effects of temperature, delta protein, and sigma factor mutations. *Biochemistry,* **34**, 8465–8473.
Kirkegaard, K., Buc, H., Spassky, A. & Wang, J. C. (1983). Mapping of single-stranded regions in duplex DNA at the sequence level: single-strand-specific cytosine methylation in RNA polymerase-promoter complexes. *Proc. Natl Acad. Sci. USA,* **80**, 2544–2548.
Kovacic, R. T. (1987). The 0°C closed complexes between *Escherichia coli* RNA polymerase and two promoters, T7-A3 and *lac* UV5. *J. Biol. Chem.* **262**, 13654–13661.
Krummel, B. & Chamberlin, M. J. (1989). RNA chain initiation by *Escherichia coli* RNA polymerase. Structural transitions of the enzyme in early ternary complexes. *Biochemistry,* **28**, 7829–7842.
Krummel, B. & Chamberlin, M. J. (1992). Structural analysis of ternary complexes of *Escherichia coli* RNA polymerase: individual complexes halted along different transcription units have distinct and unexpected biochemical properties. *J. Mol. Biol.* **225**, 221–237.
Kumar, S. A. (1981). The structure and mechanism of action of bacterial DNA-dependent RNA polymerase. *Prog. Biophys. Mol. Biol.* **38**, 165–210.
Lampe, M., Binnie, C., Schmidt, R. & Losick, R. (1988). Cloned gene encoding the delta subunit of *Bacillus subtilis* RNA polymerase. *Gene,* **67**, 13–20.
Leirmo, S. & Record, M. T., Jr (1990). Structural, thermodynamic and kinetic studies of the interaction of $E\sigma^{70}$ RNA polymerase with promoter DNA. In *Nucleic Acids and Molecular Biology* (Eckstein, F. & Lilley, D. M. J., eds), pp. 123–151, Springer-Verlag, Berlin, Heidelberg.
López de Saro, F., Woody, A.-Y. M. & Helmann, J. D. (1995). Structural analysis of the *Bacillus subtilis* δ factor: a protein polyanion which displaces RNA from RNA polymerase. *J. Mol. Biol.* **252**, 189–202.
Malhotra, A., Severinova, E. & Darst, S. A. (1996). Crystal structure of a $\sigma^{70}$ subunit fragment from *E. coli* RNA polymerase. *Cell,* **87**, 127–136.
Margalit, H., Shapiro, B. A., Nussinov, R., Owens, J. & Jernigan, R. L. (1988). Helix stability in prokaryotic promoter regions. *Biochemistry,* **27**, 5179–5188.
McClure, W. R. (1985). Mechanism and control of transcription initiation in prokaryotes. *Annu. Rev. Biochem.* **54**, 171–204.
Mecsas, J., Cowing, D. W. & Gross, C. A. (1991). Development of RNA polymerase-promoter contacts during open complex formation. *J. Mol. Biol.* **220**, 585–597.
Meier, T., Schickor, P., Wedel, A., Cellai, L. & Heumann, H. (1995). *In vitro* transcription close to the melting point of DNA: analysis of *Thermotoga maritima* RNA polymerase-promoter complexes at 75°C using chemical probes. *Nucl. Acids Res.* **23**, 988–994.
Mirel, D. B. & Chamberlin, M. J. (1989). The *Bacillus subtilis* flagellin gene (*hag*) is transcribed by the $\sigma^{28}$ form of RNA polymerase. *J. Bacteriol.* **171**, 3095–3101.
Morris, L., Cannon, W., Claverie-Martin, F., Austin, S. & Buck, M. (1994). DNA distortion and nucleation of local DNA unwinding within sigma-54 ($\sigma^N$) holoenzyme closed promoter complexes. *J. Biol. Chem.* **269**, 11563–11571.
Munson, L. & Reznikoff, W. S. (1981). Abortive initiation and long ribonucleic acid synthesis. *Biochemistry,* **20**, 2181–2085.
Newlands, J. T., Ross, W., Gosink, K. K. & Gourse, R. L. (1991). Factor-independent activation of *Escherichia coli* rRNA transcription. II. Characterization of complexes of *rrnB* P1 promoters containing or lacking the upstream activator region with *Escherichia coli* RNA polymerase. *J. Mol. Biol.* **220**, 569–583.
Nudler, E., Avetissova, E., Markovtsov, V. & Goldfarb, A. (1996). Transcription processivity: protein-DNA interactions holding together the elongation complex. *Science,* **273**, 211–217.
Ozoline, O. N. & Tsyganov, M. A. (1995). Structure of open promoter complexes with *Escherichia coli* RNA polymerase as revealed by the DNase I footprinting technique: compilation analysis. *Nucl. Acids Res.* **23**, 4533–4541.
Parekh, B. S. & Hatfield, G. W. (1996). Transcriptional activation by protein induced DNA bending: evidence for a DNA structural transmission model. *Proc. Natl Acad. Sci. USA,* **93**, 1173–1177.
Pero, J., Nelson, J. & Fox, T. D. (1975). Highly asymmetric transcription by RNA polymerase containing phage-SP01-induced polypeptides and a new host protein. *Proc. Natl Acad. Sci. USA,* **72**, 1589–1593.
Polyakov, A., Severinova, E. & Darst, S. A. (1995). Three-dimensional structure of *E. coli* core RNA polymerase: promoter binding and elongation conformations of the enzyme. *Cell,* **83**, 365–373.
Roberts, C. W. & Roberts, J. W. (1996). Base-specific recognition of the nontemplate strand of promoter DNA by *E. coli* RNA polymerase. *Cell,* **86**, 495–501.
Rojo, F., Nuez, B., Mencia, M. & Salas, M. (1993). The main early and late promoters of *Bacillus subtilis* phage ϕ29 form unstable open complexes with $\sigma^A$-RNA polymerase that are stabilized by DNA supercoiling. *Nucl. Acids Res.* **21**, 935–940.
Rong, J. C. & Helmann, J. D. (1994). Genetic and physiological studies of *Bacillus subtilis* $\sigma^A$ mutants defective in promoter melting. *J. Bacteriol.* **176**, 5218–5224.
Ross, W., Gosink, K. K., Salomon, J., Igarishi, K., Zou, C., Ishihama, A., Severinov, K. & Gourse, R. L.

(1993). A third recognition element in bacterial promoters: DNA binding by the α subunit of RNA polymerase. *Science,* **262**, 1407–1413.

Sambrook, J., Fritsch, E. F. & Maniatis, T. (1990). In *Molecular Cloning: A Laboratory Manual*. Cold Spring Harbor Laboratory Press, Cold Spring Harbor, NY.

Sasse-Dwight, S. & Gralla, J. (1991). Footprinting protein-DNA complexes *in vivo*. *Methods Enzymol.* **208**, 146–168.

Schickor, P., Metzger, W., Werel, W., Lederer, H. & Heumann, H. (1990). Topography of intermediates in transcription initiation of *E. coli*. *EMBO J.* **9**, 2215–2220.

Severinov, K., Mustaev, A., Severinova, E., Bass, I., Kashlev, M., Landick, R., Nikiforov, V., Goldfarb, A. & Darst, S. A. (1995). Assembly of functional *Escherichia coli* RNA polymerase containing β subunit fragments. *Proc. Natl Acad. Sci. USA,* **92**, 4591–4595.

Severinova, E., Severinov, K., Fenyö, D., Marr, M., Brody, E. N., Roberts, J. W., Chait, B. T. & Darst, S. A. (1996). Domain organization of the *Escherichia coli* RNA polymerase $\sigma^{70}$ subunit. *J. Mol. Biol.* **263**, 637–647.

Siebenlist, U. (1979). RNA polymerase unwinds an 11-base pair segment of a phage T7 promoter. *Nature,* **279**, 651–652.

Spassky, A., Kirkegaard, K. & Buc, H. (1985). Changes in the DNA structure of the *lacUV5* promoter during the formation of an open complex with *E. coli* RNA polymerase. *Biochemistry,* **24**, 2723–2731.

Spassky, A., Rimsky, S., Buc, H. & Busby, S. (1988). Correlation between the conformation of *Escherichia coli* −10 hexamer sequences and promoter strength: use of orthophenanthroline cuprous complex as a structural index. *EMBO J.* **7**, 1871–1879.

Suh, W.-C., Leirmo, S. & Record, M. T., Jr (1992). Roles of Mg(II) in the mechanism of formation and dissociation of open complexes between *Escherichia coli* RNA polymerase and the λ $P_R$ promoter: kinetic evidence for a second open complex requiring Mg(II). *Biochemistry,* **31**, 7815–7825.

Suh, W.-C., Ross, W. & Record, M. T., Jr (1993). Two open complexes and a requirement for $Mg^{2+}$ to open the λ$P_R$ transcription start site. *Science,* **259**, 358–361.

Travers, A. A. (1987). Structure and function of *E. coli* promoter DNA. *CRC Crit. Rev. Biochem.* **22**, 181–219.

von Hippel, P. H., Bear, D. G., Morgan, W. D. & McSwiggen, J. A. (1984). Protein-nucleic acid interactions in transcription: a molecular analysis. *Annu. Rev. Biochem.* **53**, 389–446.

Voskuil, M. I., Voepel, K. & Chambliss, G. G. (1995). The −16 region, a vital sequence for the utilization of a promoter in *Bacillus subtilis* and *Escherichia coli*. *Mol. Microbiol.* **17**, 271–279.

Werel, W., Schickor, P. & Heumann, H. (1991). Flexibility of the DNA enhances promoter affinity of *Escherichia coli* RNA polymerase. *EMBO J.* **10**, 2589–2594.

Whipple, F. W. & Sonenshein, A. L. (1992). Mechanism of initiation of transcription by *Bacillus subtilis* RNA polymerase at several promoters. *J. Mol. Biol.* **223**, 399–414.

Wu, C. W. & Goldthwait, D. A. (1969a). Studies of nucleotide binding to the ribonucleic acid polymerase by a fluorescence technique. *Biochemistry,* **8**, 4450–4458.

Wu, C. W. & Goldthwait, D. A. (1969b). Studies of nucleotide binding to the ribonucleic acid polymerase by equilibrium dialysis. *Biochemistry,* **8**, 4458–4464.

Zaychikov, E., Martin, E., Denissova, L., Kozlov, M., Markovtsov, V., Kashlev, M., Heumann, H., Nikiforov, V., Goldfarb, A. & Mustaev, A. (1996). Mapping of catalytic residues in the RNA polymerase active center. *Science,* **273**, 107–109.

***Edited by M. Gottesman***

*(Received 18 September 1996; received in revised form 5 December 1996; accepted 5 December 1996)*